R. W. Cole
R. I. Potter
C. C. Lin
K. L. Deckert
E. P. Valstyn

Numerical Analysis of the Shielded Magnetoresistive Head

Abstract: Numerical computations for the shielded magnetoresistive head are reported and compared with previous analytic and experimental results. Linear resolution is found to be essentially the same as for inductive heads. Output amplitude is in the range 50 to 175 V per meter track width for a sense current density of 5×10^{10} A/m^2.

Introduction

The trend toward increased density in digital magnetic recording has led to miniaturized single- and multi-turn recording heads fabricated by film technology [1]. A shielded magnetoresistive (MR) head [2], which physically is about the size of a single-turn inductive head, can also be considered for high density recording. The shields, which are pieces of magnetic material located near both sides of the vertical MR stripe, increase the linear resolution of the device to that obtained from inductive heads. This resolution is substantially beyond that of the unshielded MR head described by Hunt [3] and analyzed numerically by Anderson, et al. [4]. The MR head is a read-only device, in basic form, but the various parts (MR stripe, magnetic bias conductors, and shields) can be combined in a wide variety of ways to form a composite read and write structure. The MR stripe also can be placed within the gap of a conventional head [5]. The peak-to-peak output of the MR head is about 100 μV per μm of track width, or roughly two orders of magnitude greater than that of the single-turn head.

In this paper we report the results of numerical calculations for the shielded MR head and compare them to experimental results and an approximate analytic treatment given previously by one of us [2]. We calculate pulse shapes, output amplitudes, and resistivity (or magnetization) throughout the shielded MR stripe. We also investigate the nonlinear response caused by the quadratic $\Delta\rho$ versus $H_{\text{sig}} + H_{\text{bias}}$ relation, an aspect of the problem that the linearized analytic treatment ignores. The approximate analytic treatment, these more detailed numerical results, and the experimental data are in reasonable agreement wherever comparisons are appropriate.

Shielded MR head geometry

A cross section of the head considered throughout most of this paper is shown in Fig. 1. Because the analytic treatment and experimental results are for the case $s \gg g$, where s is the length of each shield along the track direction, we choose $s = 16$ μm and restrict $\bar{x} \equiv vt$ to the interval $0 \leq \bar{x} \leq 5$ μm. The shield height is 32 μm for all computations.

An arctangent transition with transition length parameter a in the thin medium at $y = -d$ is represented [6] by a line charge at $(x, y) = (\bar{x}, -d - a)$. This simplification

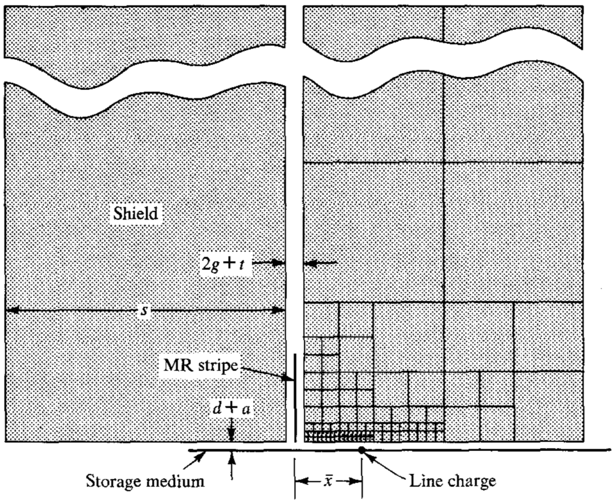

Figure 1 Shielded MR head geometry with nonuniformly sized volume elements shown for right-hand shield only. Note that "gap length" g means the stripe-to-shield distance for MR heads, and the pole-piece to pole-piece distance for inductive heads.

causes no loss of generality, because the fields [7] produced by these two transitions are identical for $y > -d$. As for inductive heads, the output pulse of the MR head depends only on the sum $d + a$.

Two current conductors are placed between the shields, one on each side of the MR stripe. They carry oppositely directed currents and bias the MR stripe to one side of its bell-shaped $\Delta\rho$ versus H curve with $\langle \Delta\rho(y) \rangle_{av} \simeq -\frac{1}{2}\Delta\rho_{max}$. These conductors are not shown in Fig. 1.

The MR stripe extends from $y = 0$ to $y = L = 5$ μm in the vertical direction and is 200 Å thick. The easy axis, current-density vector, and coordinate z axis are all normal to the plane of the figure. According to simple theory the optimum MR stripe height is about $L = (tg\mu_r/2)^{\frac{1}{2}}$, where $2g + t$ is the shield-to-shield separation and μ_r the relative permeability, taken as 1000 for all calculations. The value $L = 5$ μm is somewhat larger than the value given by this criterion but the choice is not (and from a practical standpoint must not be) critical. Head efficiency suffers if $L \gg (tg\mu_r/2)^{\frac{1}{2}}$. The choice that t be 200 Å is for the sake of convenience; provided that $t \ll g$, this parameter has negligible effect on head resolution. It does, however, provide one means of controlling flux density within the stripe and preventing stripe saturation. Flux density is proportional to $\mu_0 M_r \delta / t$, where $M_r\delta$ is the strength of the storage medium transition.

The remaining parameters are chosen to afford a comparison with previous results and are listed here along with those discussed above:

$$d + a = 0.5, 0.82, \text{ and } 1.0\ \mu\text{m},$$

$$g = 0.25, 0.5, 0.75, \text{ and } 1.0\ \mu\text{m},$$

$$t = 200\ \text{Å},$$

$$L = 5\ \mu\text{m},$$

$$\mu_r = 1000,$$

$$\delta = 100 \text{ and } 500\ \text{Å, and}$$

$$M_r = 800\ \text{emu/cm}^3\ (8 \times 10^5\ \text{A/m}).$$

Many of these parameters enter additively or multiplicatively, and therefore the results given below can be interpreted in many ways. They also can be scaled.

Computational procedure

A discussion of the computer program used to determine the field intensity within the MR stripe is given elsewhere [2]. Briefly, the magnetic material is divided into N interacting uniformly magnetized volume elements immersed in an applied field, and the resulting $2N$ linear equations are solved for the $2N$ unknown magnetization components. Here, the applied field has two sources: the bias conductors, located on both sides of the MR stripe, and the arctangent transition, located within the thin storage medium. The output pulse is obtained by repeating the computation for a large number of transition locations $\bar{x}$, because reciprocity does not apply. The signal voltage is

$$e(x) = I_s \Delta R(\bar{x}), \tag{1}$$

where I_s is the sense current and ΔR is the change in stripe resistance due to the presence of the transition,

$$\Delta R(\bar{x}) = W\left\{t \int_0^L \frac{dy}{\rho[H(y;\bar{x})]}\right\}^{-1} - R_0$$
$$\simeq \frac{W}{tL} \langle \rho(y;\bar{x}) \rangle_{av} - R_0, \tag{2}$$

and where R_0 is the resistance in the absence of the transition. We represent the stripe resistivity by

$$\rho = \begin{cases} \rho_0 + \Delta\rho_{max}\left[1 - \dfrac{H_x^2 + H_y^2}{H_k^2}\right], & H_x^2 + H_y^2 \le H_k^2; \\ \rho_0 & , H_x^2 + H_y^2 > H_k^2, \end{cases} \tag{3}$$

where H_k is the anisotropy field. Both field components are kept in ρ because shape anisotropy is implicitly included in the numerical calculation. The sign of the storage medium transition is chosen so that H_{sig} opposes H_{bias}.

A nonuniform grid is used as shown in Fig. 1, with both shields subdivided in an identical manner. The stripe is subdivided into 20 rectangular volume elements when $s = 16$ μm. The program is run in the nonsaturation mode

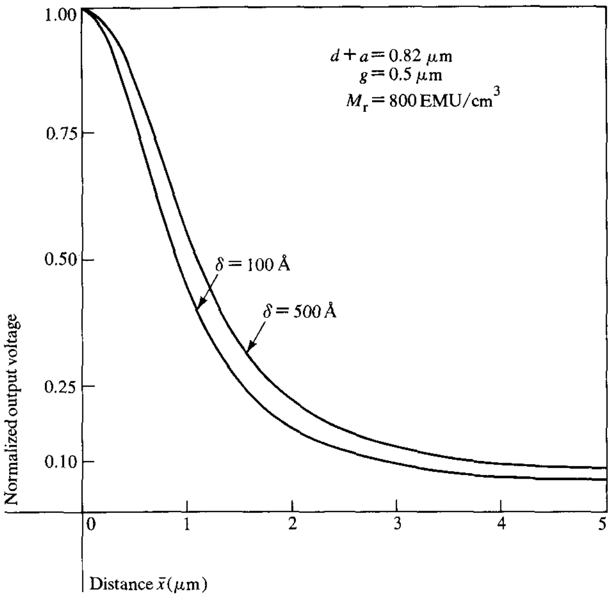

Figure 2 Shielded MR head output pulse for two storage medium $M_r\delta$ products. Pulse shapes are different because of the quadratic $\Delta\rho$ versus H response of the magnetoresistive stripe.

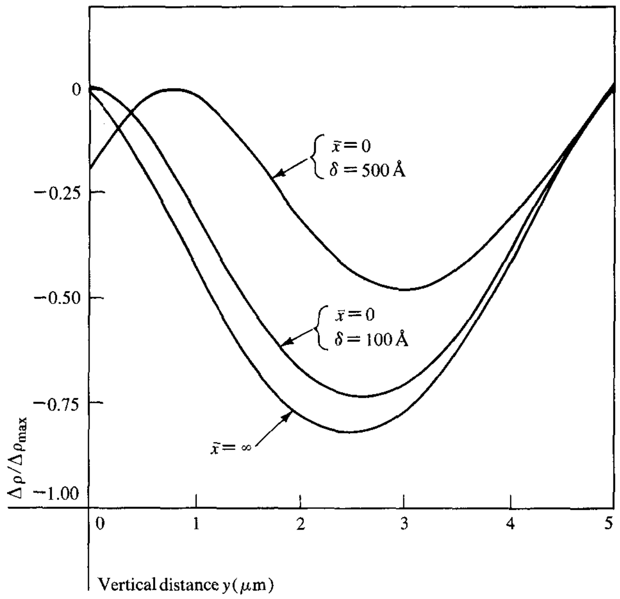

Figure 3 Stripe resistivity versus distance measured vertically from shield faces. Curve labeled $\bar{x}\rightarrow\infty$ indicates magnetic bias condition. Curves labeled $\bar{x}=0$ show resistivity when transition is nearest stripe and correspond to the output pulses of Fig. 2.

with $\chi = M_s/H_k = 999$ (mks units) describing the magnetic material. For all computations reported here $|M(i)|_{max} < M_s$, where $M(i)$ is the magnetization of the ith volume element.

As a test of the reliability of these computations, the case where shield length $s = 0.5\ \mu$m is considered, in part because the small cross-sectional area of this shield makes a refinement of the grid feasible. It is believed that thin shields with few volume elements of a given size would be more sensitive to a grid refinement than thick ones, but no attempt to verify this by experimentation with the 16-μm grid was made. The basic 0.5-μm grid consists of 40 volume elements for the stripe and 62 0.5 μm × 0.5 μm, or four 0.25 μm × 0.25 μm and 16 0.125 μm × 0.125 μm volume elements for each shield. The shield height remains 32 μm. The refined grid has all volume elements within the shields divided into quarters. The comparison gives, for example, with remaining parameters as in Fig. 4, $\Delta e(1) = 0.004$, $\Delta e(3) = -0.001$, and $\Delta e(5) = -0.009$, where $\Delta e \equiv e - e_{refined}$, with both pulses normalized to unity at $\bar{x} = 0$. This amounts to less than a one percent change in $e(\bar{x})$ in the region where $e(\bar{x})$ is down to one-half its peak value. The pulse skirt, however, changes about 10 percent (or one percent of the total pulse height) at $\bar{x} = 5\ \mu$m. In general, an inadequate grid first manifests itself in the pulse skirt.

Results

Shown in Fig. 2 are pulses for $\delta = 100$ and 500 Å, both for $d + a = 0.82\ \mu$m and $g = 0.5\ \mu$m. Corresponding stripe resistivities are shown in Fig. 3 for $\bar{x} = 0$ and as $\bar{x} \rightarrow \infty$ (or $\delta = 0$). The signal voltage for a given $\bar{x}$ is proportional to the area bounded by the curves $\rho(y; \bar{x})$ and $\rho(y, \infty)$. Shown in Fig. 3 are the curves $\rho(y; 0)$ and $\rho(y; \infty)$ only; they indicate the peak signal and those portions of the stripe that are most active in generating it.

The field from the $\delta = 500$ Å medium is so strong that the nearer portion of the stripe is driven through $H_{total} = H_{sig} + H_{bias} = 0$ and onto the opposite side of the $\Delta\rho$ versus H_{total} curve, as indicated by Fig. 3, with a corresponding broadening of the pulse as shown in Fig. 2. A further increase in transition strength would cause the pulse of this polarity to exhibit two maxima. The choice $M_r\delta$ = 800 emu/cm^3 × 100 Å and t = 200 Å is more reasonable and gives a peak-to-peak isolated pulse output of 57 μV per μm of track width, assuming $\Delta\rho_{max} = 7 \times 10^{-9}$ Ω-m [8] and a reasonable [9] sense-current density $J = 5 \times 10^{10}$ A/m^2 (5 mA for $L = 5\ \mu$m, $t = 200$ Å). The output for the $\delta = 500$ Å case is 175 μV per μm of track width.

The analytic model [2] predicts an output amplitude

$$e_{pp} = (4\sqrt{2}/\pi)\ JW\ \Delta\rho_{max} \frac{M_r\delta}{M_s t} \times \left[\tan^{-1}\frac{g}{d+a} - \frac{d+a}{2g}\ln\frac{g^2 + (d+a)^2}{(d+a)^2}\right] \qquad (4)$$

when t and δ are small compared to g and $d + a$. It is a linearized small-signal model, in which it is assumed that the bias field and $(d\rho/dH)_{H_{bias}}$ are uniform throughout the stripe (not true when generated by adjacent conduc-

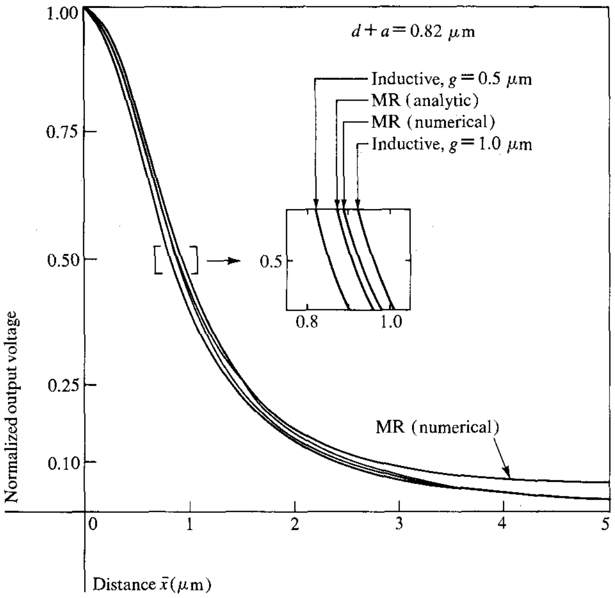

Figure 4 Comparison of the $g = 0.5$ μm MR head output pulse as computed analytically [2] and numerically (this work). Also shown are two inductive-head pulses, where g is the pole-face to pole-face distance, as computed according to the approximation of Karlquist. These computations indicate that the effective gap length of the shielded MR head is less than the distance between shields.

tors), that $B_{sig} = 0$ at $y = L$ (a boundary condition well supported by the numerical calculations), and that $\langle B_{sig}(y) \rangle = \frac{1}{2} B_{sig}(0)$. This model predicts $e_{pp} = 94$ V/m for the $\delta = 100$ Å case described above.

Most linear density predictions rest upon superposition of isolated pulses. We compare in Fig. 4, therefore, the isolated pulse for the $\delta = 100$ Å case above as given by the analytic model and this numerical computation. Also shown is the inductive-head pulse for gap length equal to the shield-to-shield spacing, $2g + t$, and for half this value. The MR head pulse shape for other values of g and $d + a$ is similar to that of Fig. 2 when stripe saturation does not occur. Full pulse widths, at half maximum, P_{50}, obtained by numerical computation for several additional cases, are listed in Table 1. The −6 dB point on the "all-ones" roll-off curve is approximately given by $1.39/P_{50}$ [10]. This density is about 7400 flux reversals per cm for the $d + a = 0.82$ μm and $g = 0.5$ μm case.

These numerical calculations indicate that the expression of Bonyhard, Davies, and Middleton (BDM) [11],

$$P_{50} = [g^2 + 4(d + a)^2]^{\frac{1}{2}}, \quad (5)$$

used by Potter [2] to predict the pulse width for an MR head with shield-to-shield spacing $2g + t$ and with $t \ll g$ gives somewhat optimistic results. For instance, P_{50} (BDM) = 1.714 μm, whereas P_{50} (numerical) = 1.87 μm when g = 0.5 μm, $d + a = 0.82$ μm, and $\delta = 100$ Å.

Table 1 MR head pulse width P_{50} for $M_r = 800$ emu/cm^3 (8×10^5 A/m), $\delta = 100$ Å, and several combinations of g and $d + a$. All distances are in μm.

g	$d + a = 0.5$	$d + a = 0.82$	$d + a = 1.0$
0.25	1.16	1.80	2.18
0.5	1.29	1.87	2.21
0.75	1.53	2.05	2.36
1.0	1.81	2.27	2.56

On the other hand, the value $d + a = 0.82$ μm is slightly pessimistic for the optimum storage medium. It comes from scaling the self-consistent results of Potter and Schmulian [12], which results in a medium with the $M_r\delta$ product at least twice as great as is desirable for use with the MR head. This leads to stripe saturation (the $\delta = 500$ Å case above), a problem that could be solved by increasing stripe thickness t, but is better solved by reducing $M_r\delta$. Note that the storage medium used in Potter's experiments has an equivalent thickness of about 260 Å if $M_r = 800$ emu/cm^3 (8×10^5 A/m) and a coercive force $H_c = 480$ Oe (3.8×10^4 A/m). Thus, for this medium his relationship $a(d) = 2.26d$ is pessimistic but apparently, from the agreement with experiment, largely cancelled by the use of the BDM expression.

In conclusion, we find that previous analytical and experimental results are in reasonable agreement with these more detailed numerical computations. The behavior of the shielded MR head for realistic bias conditions and signal field strengths was studied and found acceptable. Current conductors placed adjacent to the MR stripe have been shown to be one satisfactory method of providing magnetic bias. The previously estimated areal density of 1.6×10^7 flux reversals per square centimeter [2] is reasonable, based on scaling these numerical results.

References and note

1. See, for instance, E. P. Valstyn and L. F. Shew, *IEEE Trans. Magnetics* **MAG-9,** 317 (1973); J. P. Lazzari, *IEEE Trans. Magnetics* **MAG-9,** 322 (1973).
2. R. I. Potter, Paper 2.4 of 1974 Intermag Conference, and to be published in September 1974 issue of *IEEE Trans. Magnetics.*
3. R. P. Hunt, *IEEE Trans. Magnetics* **MAG-7,** 150 (1971); U.S. Patent 3,493,694.
4. R. L. Anderson, C. H. Bajorek, and D. A. Thompson, *AIP Conference Proceedings on Magnetism and Magnetic Materials,* **10,** 1445 (1972).
5. F. W. Gorter and J. A. L. Potgiesser, Paper 31.6 of 1974 Intermag Conference, and to be published in September 1974 issue of *IEEE Trans. Magnetics.*
6. We chose the coordinate system so that y is positive within the head in order to simplify the one-dimensional analytic head efficiency calculations mentioned here and described more fully in [2].
7. R. I. Potter, *J. Appl. Phys.* **41,** 1647 (1970).
8. S. Krongelb, *J. Electronic Materials* **2,** 227 (1973).

9. C. H. Bajorek and F. A. Mayadas, *AIP Conference Proceedings on Magnetism and Magnetic Materials*, **10**, 212 (1972).
10. R. L. Comstock and M. L. Williams, *IEEE Trans. Magnetics* **MAG-9**, 342 (1973). The factor 1.39 comes from recognizing that the root of sinh $x = 2x$ is $x \equiv \pi p/(2s) = 2.18$ (their notation).
11. P. I. Bonyhard, A. V. Davies, and B. K. Middleton, *IEEE Trans. Magnetics* **MAG-2**, 1 (1966).
12. R. I. Potter and R. J. Schmulian, *IEEE Trans. Magnetics* **MAG-7**, 873 (1971).

Received May 8, 1974

R. W. Cole, K. L. Deckert, C. C. Lin, and E. P. Valstyn are located in the IBM General Products Division Laboratory in San Jose, California 95193. R. I. Potter is located in the IBM Research Division Laboratory in San Jose, California 95193.